JOC The Journal of Organic Chemistry

Article

Water-Soluble Molecularly Imprinted Nanoparticle Receptors with Hydrogen-Bond-Assisted Hydrophobic Binding

Md Arifuzzaman, and Yan Zhao

J. Org. Chem., **Just Accepted Manuscript** • DOI: 10.1021/acs.joc.6b01191 • Publication Date (Web): 27 Jul 2016

ACS Publications

The Journal of Organic Chemistry is published by the American Chemical Society.
1155 Sixteenth Street N.W., Washington, DC 20036

Water-Soluble Molecularly Imprinted Nanoparticle Receptors with Hydrogen-Bond-Assisted Hydrophobic Binding

*MD Arifuzzaman and Yan Zhao**

Department of Chemistry, Iowa State University, Ames, Iowa 50011-3111

zhaoy@iastate.edu

RECEIVED DATE

ABSTRACT. Molecularly imprinted nanoparticles (MINPs) were prepared when surfactants with a tripropargylammonium headgroup and a methacrylate-functionalized hydrophobic tail were cross-linked in the micelle form on the surface and in the core in the presence of hydrophobic template molecules. With the surfactants containing an amide bond near the headgroup, the MINPs had a layer of hydrogen-bonding groups in the interior that strongly influenced their molecular recognition. Templates/guests with strong hydrogen-bonding groups in the midsection of the molecule benefited most, especially if the hydrophobe of the template could penetrate the amide layer to reach the hydrophobic core of the cross-linked micelles. The location and the orientation of the hydrophilic groups were also important, as they determined how the template interacted with the surfactant micelles and, ultimately, with the MINP receptors.

Introduction

Molecular recognition is at the heart of nearly every biological process, be it enzymatic catalysis, ligand–receptor binding, selective transport of nutrients across membranes, or gene expression. To recognize a guest molecule with high affinity and selectivity, the host needs to possess a binding interface complementary to the guest in size, shape, and distribution of functional groups. Over the last several decades, a great number of synthetic hosts with such features have been prepared, often through molecular synthesis.[1-3] The benefit of molecular synthesis is that well-defined host molecules can be obtained and numerous methods (spectroscopic or otherwise) may be used to study the host–guest complexes. On the other hand, molecular hosts, typically larger and more complex than the guest molecules, require significant synthetic efforts to prepare. For guest molecules with complex functionality and shape, designing hosts with good (let alone perfect) complementarity can be extremely challenging.

Molecular imprinting is a conceptually different method to create guest-complementary hosts.[4-14] In a typical procedure, free radical polymerization is induced in a mixture of template molecules, functional monomers (FMs) that bind the templates by noncovalent or covalent bonds, and cross-linkers to maintain rigidity of the resulting polymer. The cross-linked material, after removal of the templates by washing or bond cleavage, is left with cavities complementary to the templates and thus considered "molecularly imprinted" with the templates. The method has been adopted by numerous researchers for a wide range of applications in molecular recognition, separation, enzyme-mimetic catalysis, and chemical sensing. In addition to traditional macroporous polymers, imprinting could occur on surface and even unimolecularly within dendrimers.[15,16]

An extremely attractive feature of molecular imprinting is the simplicity in the design and preparation of molecularly imprinted polymers (MIPs). Free radical polymerization is easy to perform and guest-complementary binding sites are created by the imprinting process, without the need of custom design for each individual guest. As a result, the method can be used by scientists without substantial training in supramolecular chemistry and organic synthesis.

Nonetheless, there remain a number of challenges in this technique. For example, it is generally accepted that binding sites in MIPs are heterogeneous and poorly defined in structure.[4-6,8-12,17,18] Conventional MIPs are intractable macroporous polymers and limited methods are available to understand their structure and binding properties.[19] Template molecules are frequently trapped deep inside the cross-linked and polymeric matrix and difficult to be removed. Although soluble nanoparticle MIPs have been reported,[20-28] aqueous compatibility remains a challenge.[29]

We have been interested in the design and synthesis of functional receptors through biomimetic strategies.[30,31] Recently, we reported a method to imprint within cross-linked surfactant micelles to create molecularly imprinted nanoparticles (MINPs). Our method worked well for a number of water-soluble molecules including bile salt derivatives,[32] aromatic carboxylates and sulfonates,[33-35] and nonsteroidal anti-inflammatory drugs (NSAIDs).[36] In addition, we could install specific functional groups in the MINP binding site and chemically modify the functional groups.[34] Because MINPs are fully soluble in water and similar to protein in size (40–60 KD in MW), we could study their binding by techniques used for molecular receptors such as fluorescence titration, isothermal titration calorimetry (ITC), and chemical derivatization. They are similar to water-soluble proteins in topology, having a hydrophilic exterior and a hydrophobic core with guest-complementary binding sites.

The most important building block in the MINP synthesis is the cross-linkable surfactant that serves multiple roles in the molecular imprinting. Its micellization defines the boundary for polymerization and cross-linking, and enables the highly cross-linked MINPs to be fully soluble due to their nanosize and solubilizing ligands on the surface. It serves as the FM to bind the template (mainly through hydrophobic and electrostatic interactions), as well as one of the cross-linkers to maintain integrity of the binding site. Its alkynyl headgroup allows facile surface-decoration of the nanoparticles with different functional groups.

In this paper, we report two new cross-linkable surfactants synthesized from more readily available, less expensive starting materials than the previously reported surfactant. Importantly, their amide group within the structure enables the surfactants to interact with the template or guest molecules by hydrogen

bonds, in addition to hydrophobic and electrostatic interactions. Our study also yielded interesting insight into how the position of the amide bond affects the imprinting process and molecular recognition of the MINPs. The binding pockets in the MINPs were found to be highly discriminating, even toward very similar guest molecules.

Results and Discussion

Design, Syntheses, and Characterization of Cross-Linkable Surfactants. Our previously reported MINPs were prepared using cross-linkable surfactant **1**.[32-34,36] Its tripropargylammonium headgroup enables facile cross-linking and decoration of the micellar surface by the alkyne–azide click reaction (Scheme 1).[37,38] The hydrophobic C12 chain provides necessary amphiphilicity to the surfactant. The methacrylate allows the surfactant to be cross-linked in the core (with DVB) by free radical polymerization. Dynamic light scattering (DLS) showed that each MINP contained approximately 50 (cross-linked) surfactant molecules. Thus, with a surfactant/template ratio of 50:1 in the preparation, the MINPs obtained typically have on average one binding site per nanoparticle. Doubling the amount of template resulted in two binding sites per nanoparticle, as demonstrated in a previous study.[32]

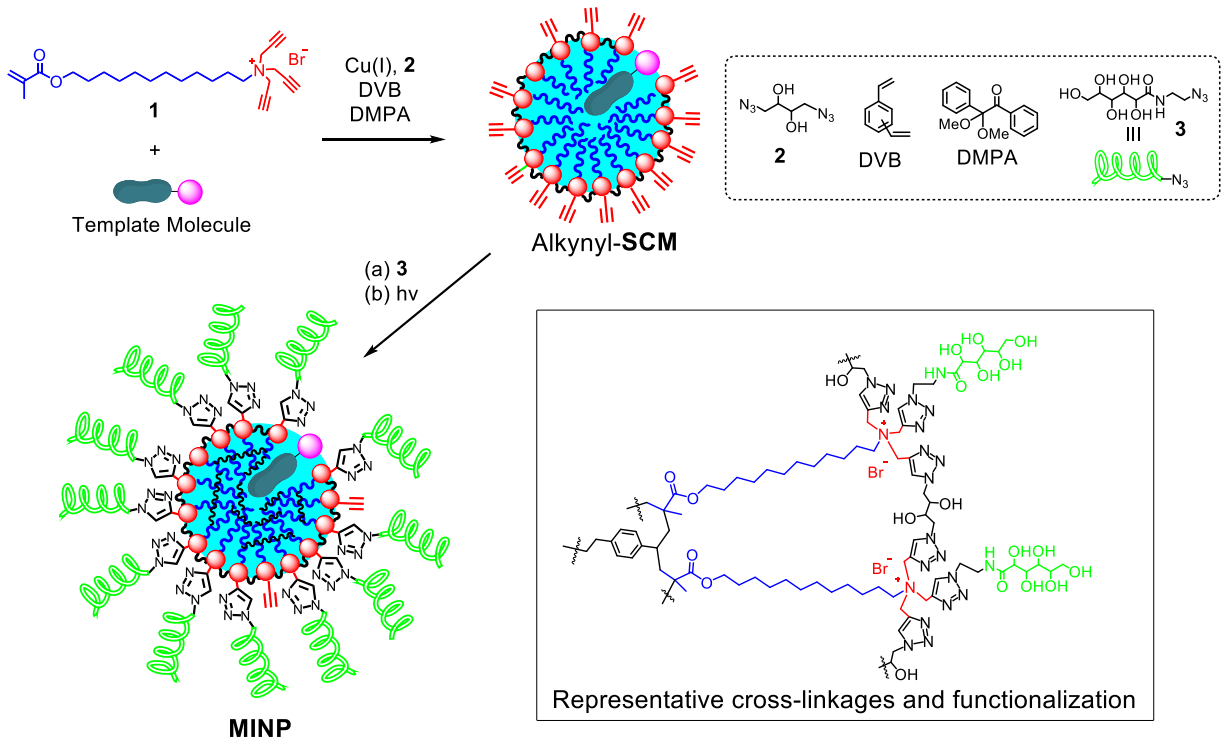

Scheme 1. Preparation of MINP by surface-cross-linking of micelle of **1**, surface decoration of resulting alkynyl-surface-cross-linked micelle (alkynyl-SCM) by ligand **3**, and core-cross-linking of the resulting material to afford MINP with an internal binding site complementary to the template molecule.

Surfactant **1** was synthesized in a three-step reaction from 1,12-dodecanediol—i.e., monomethacrylation of the diol, conversion of the remaining alcohol to trifluoromethansulfonate (triflate) with triflic anhydride, and nucleophilic substitution of the triflate with tripropargylamine. Although the synthetic route is short, it requires two expensive reagents (i.e., triflic anhydride and tripropargylamine), and a final ion exchange must be done to replace triflate with a more soluble anion such as bromide.[32]

In this study, we designed two new cross-linkable surfactants prepared from commercially available δ-undecalactone (Scheme 2). Ring opening of the lactone by 5 equiv ethylenediamine or butylenediamine at room temperature afforded amine **5a** and **5b**, respectively. The amine could be used in the next step simply after removing the excess ethylenediamine or butylenediamine by co-evaporation with methanol under vacuum. Propargylation of **5a** or **5b** occurred readily in acetonitrile with propargyl bromide and sodium bicarbonate, thus avoiding the more expensive tripropargylamine. The ammonium salt (**6a** or **6b**) was treated with methacryloyl chloride, which converted the hydroxyl group on the hydrophobic tail into methacrylate to yield the final surfactant (**4a** and **4b**).

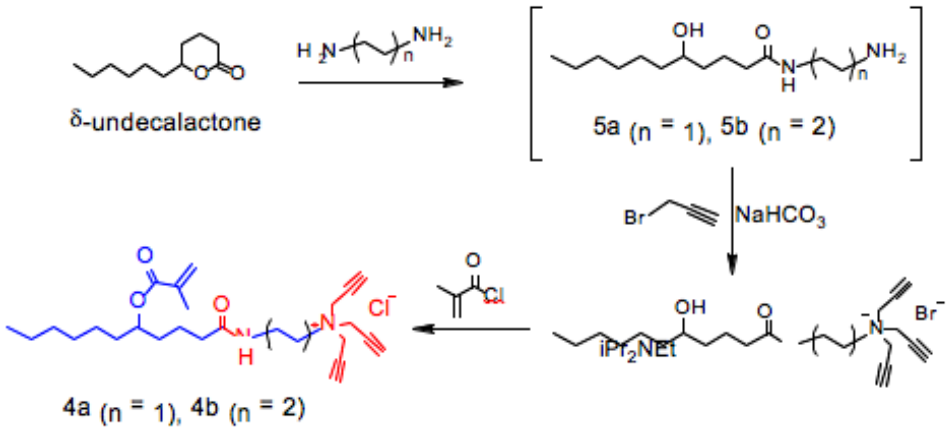

Scheme 2. Syntheses of cross-linkable surfactants **4a** and **4b** from δ-undecalactone.

In addition to easier synthesis from less expensive starting materials, the new surfactants (**4a** and **4b**) have an internal amide bond on the hydrophobic backbone. Although one might think hydrogen bonds in aqueous solution does not contribute too much to guest-binding, the hydrogen bonds in our case are located within the micelle and ultimately within the hydrophobic core of the MINP. The local hydrophobicity around the amide bonds should increase their strength and make them potentially important to guest binding. Surfactants **4a** and **4b** differ in the number of carbons between the amide bond and the tripropargylammonium headgroup. Because the ammonium headgroup has to stay on the surface of the micelle/MINP, in contact with water, the hydrogen bonds are deeper within the hydrophobic core of $MINP_{\mathbf{4b}}$ (i.e., MINP prepared with **4b** as the cross-linkable surfactant) than within the core of $MINP_{\mathbf{4a}}$.

One of the most important properties of a surfactant is its critical micelle concentration (CMC), above which micelles begin to form. To determine the CMC, we used the method of pyrene solubilization.[39] The method in our hands afforded similar CMC values as those determined from the reduction of surface tension for analogous surfactants.[37,40] Typically, we prepared aqueous solutions of a surfactant in different concentrations, with 0.1 μM of pyrene in water. Pyrene is an environmentally sensitive fluorescent probe with five vibronic bands. The first band (I_1) near 372 nm becomes stronger in a more polar environment and the third (I_3) near 384 nm changes little. The I_3/I_1 ratio thus increases with decreasing environmental polarity.

As shown in Figure 1a,b, the I_3/I_1 ratio initially showed very small change but began to rise sharply as the surfactant concentration increased beyond a certain point. The probe apparently was in the aqueous phase in the beginning but entered a nonpolar environment at higher surfactant concentrations. The inflection point of the curve normally is considered the CMC of the surfactant, and was 0.41 mM for **4a** and 0.27 mM for **4b**. The lower CMC for the latter was reasonable given its higher hydrophobicity. It is also possible that the deeper location of the amide in the hydrophobic core of the micelle strengthens the hydrogen bonds among the amide groups and stabilizes the micelle in the meantime.

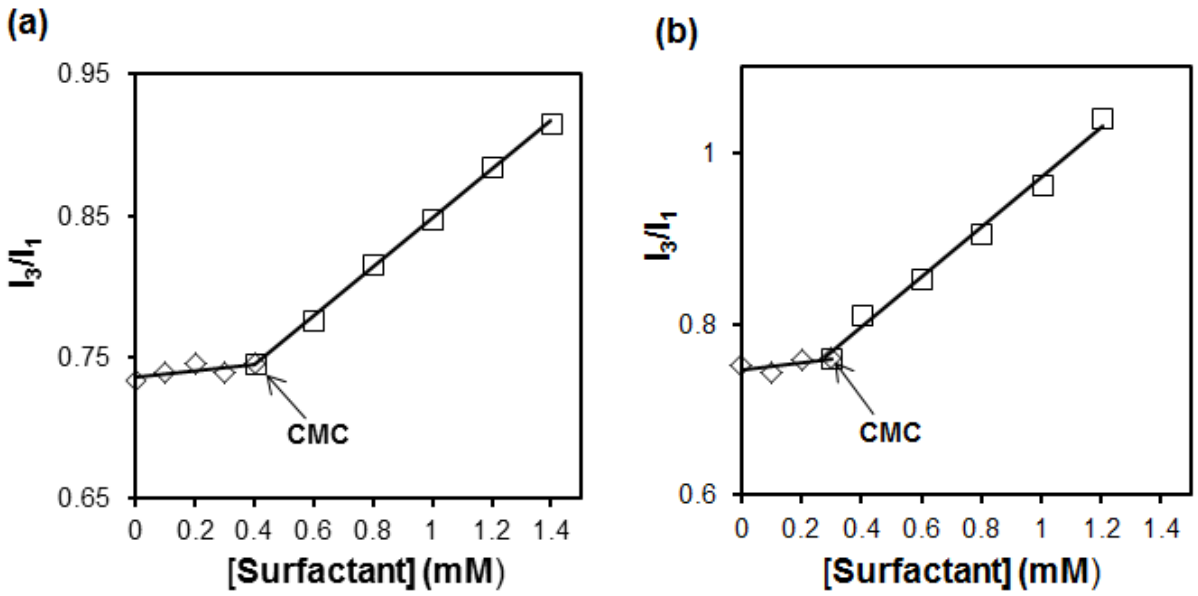

Figure 1. (a) Pyrene I_3/I_1 ratio as a function of [**4a**]. (b) Pyrene I_3/I_1 ratio as a function of [**4b**]. [pyrene] = 0.1 μM

Contribution of Hydrogen-Bonds to Molecular Imprinting and Guest-Binding. To understand whether the amide group in **4a** and **4b** could enhance the guest binding of MINPs by hydrogen bonds, we designed three template molecules **7**–**9** whose syntheses are shown in Scheme 3. The templates all have a fluorescent dansyl group connected to an aminobenzoate derivative through sulfonamide. The benefit of using dansyl as the hydrophobic group is its environmentally sensitive emission that enables us to study the binding by fluorescence spectroscopy (vide infra), in addition to ITC. The choice of having a carboxylate in the template is two-fold. First, its anionic nature makes it electrostatically attracted to the cationic micelle and the final MINP. Second, incomplete template removal is frequently a problem in conventional imprinting.[19] Being ionic, the carboxylate has to stay on the surface of the micelle to be solvated by water, while the dansyl group prefers to stay inside the micelle due to its hydrophobicity. The carboxylate then serves as an anchor to keep the template near the micelle surface, making the binding site easily vacated after imprinting and readily accessible to guest molecules during re-binding.[32]

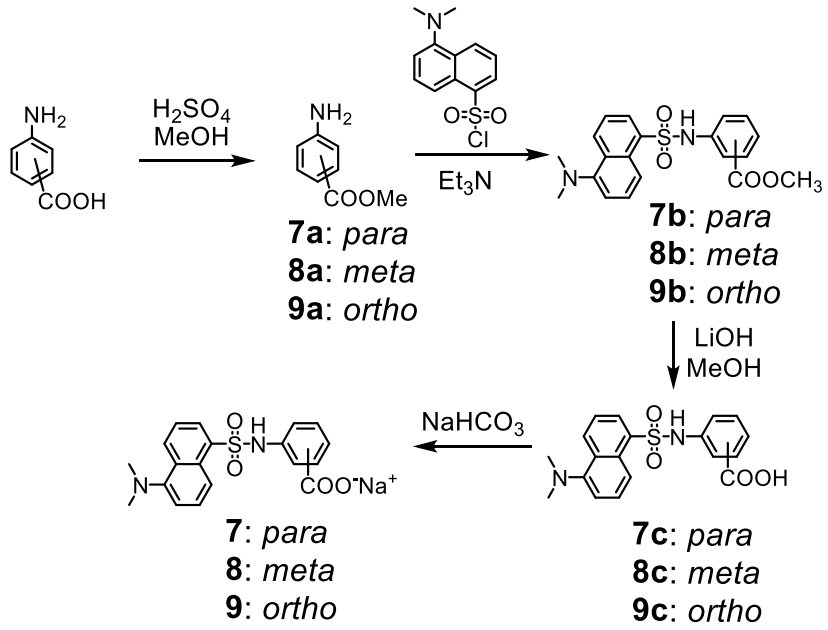

Scheme 3. Syntheses of templates **7**–**9** from the corresponding aminobenzoic acids.

The three templates differ in the substitution of the aminobenzoate moiety. The different substitutions keep the carboxylate and the sulfonamide in different distances. Since we expect the carboxylate of the template to interact with the ammonium headgroup of the surfactant electrostatically and the sulfonamide of the template with the amide of the surfactant by hydrogen bonds, it might be beneficial to match the distance between the ionic and the hydrogen-bonding functional group in the two.

Preparation of MINPs followed Scheme 1 and detailed procedures are found in the Experimental Section. In general, the surface-cross-linking and core-polymerization were monitored by ^{1}H NMR spectroscopy and DLS.[32] ^{1}H NMR spectroscopy normally shows broadening/disappearance of characteristic signals as the surfactant and DVB (core-cross-linker) undergo free radical polymerization. DLS gives the size of the nanoparticles and allows us to estimate the molecular weight of the MINP and the number of (cross-linked) surfactants within a MINP. The surface-cross-linked micelles previously were characterized also by transmission electron microscopy (TEM) and mass spectrometry (after cleaving the surface-cross-linkages).[37]

Figure 2a shows the emission spectra of template **7** upon titration with MINP$_1$(**7**), i.e., MINP prepared with cross-linkable surfactant **1** and template **7**. The addition of MINP caused a large blue shift in the emission maximum of dansyl from ~550 to ~470 nm, while greatly enhancing the emission

intensity. Dansyl is known to fluoresce weakly in water but strongly in nonpolar environments; its emission wavelength typically increases with increasing environmental polarity.[41] The blue shift and stronger emission indicate that the probe entered a nonpolar microenvironment during titration, in agreement with its binding by MINP. The fluorescence data fit well to a 1:1 binding model and afforded a binding constant (K_a) of (15.3 ± 1.1) × 10^4 M^{-1} in water (Figure 2b).

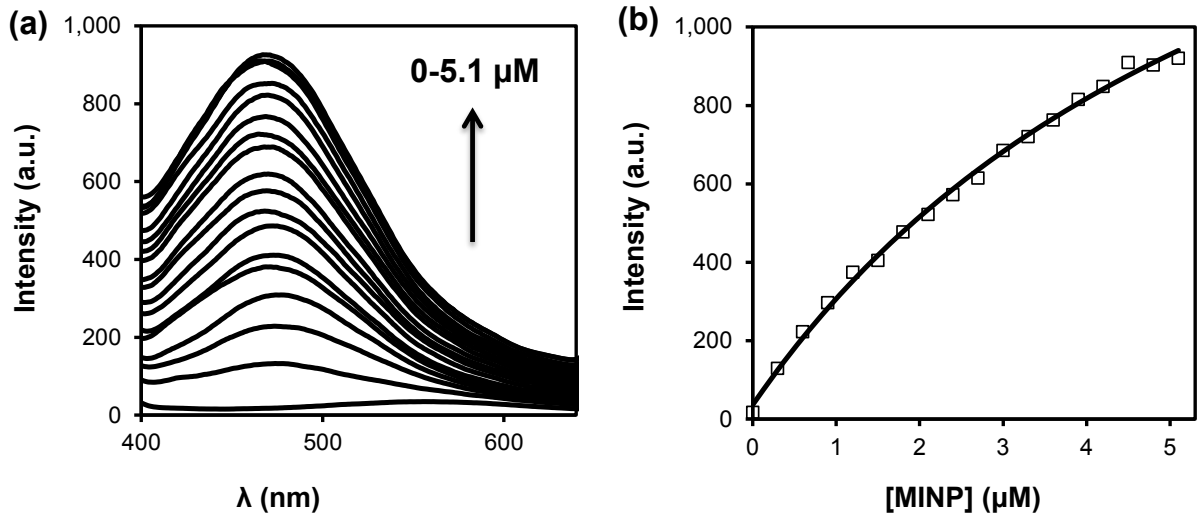

Figure 2. (a) Emission spectra of compound **7** in the presence of 0–5.1 μM of $MINP_1$(**7**) in Millipore water. [**7**] = 0.2 μM. λ_{ex} = 340 nm. (b) Nonlinear least squares curve fitting of the fluorescence intensity at 463 nm to a 1:1 binding isotherm.

The binding was also studied by ITC, one of the most reliable ways to study intermolecular interactions.[42] By measuring the heat change during the titration, ITC yields a wealth of information on the binding, including the binding constant (K_a), enthalpy (ΔH), and the number of binding sites per particle (N). The binding free energy (ΔG) can be calculated from K_a using equation $-\Delta G = RT\ln(K_a)$, and ΔS can be calculated from ΔG and ΔH. As shown in Figure 3, the binding exhibited a negative/favorable enthalpy, with K_a = (12.8 ± 0.3) × 10^4 M^{-1}. The binding constant agreed well with the value obtained by fluorescence titration. The average number of binding site per nanoparticle (N) was 1.3 ± 0.2, also consistent with the 1:1 binding model.

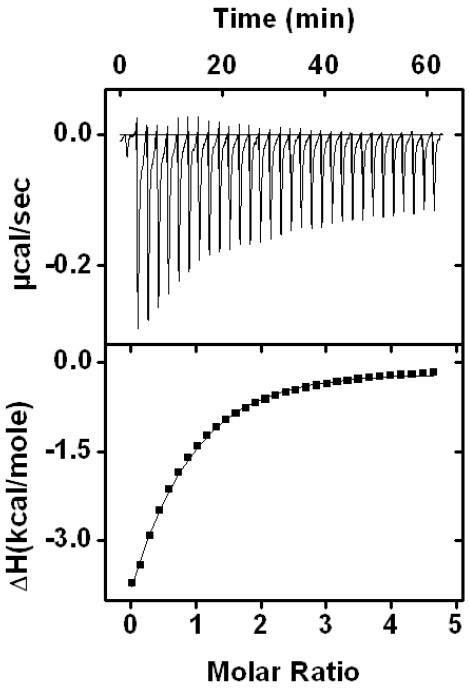

Figure 3. ITC curve obtained at 298.15 K from titration of $MINP_1$(**7**) with **7** in water. $MINP_1$(**7**) = 10 µM in the cell. The concentration of **7** in the syringe was 0.2 mM.

Table 1 summarizes the binding data obtained for the three model templates by different MINPs. Entries 1–3 compare the effectiveness of molecular imprinting of the same template (**7**) by the three different surfactants. The binding data, whether those from ITC or fluorescence titration, all point to **4a** as the most effective cross-linkable surfactant among the three. $MINP_{4a}$(**7**) bound template **7** nearly one order of magnitude stronger than $MINP_1$(**7**) prepared from the original cross-linkable surfactant. Although $MINP_{4b}$(**7**) showed weaker binding than $MINP_{4a}$(**7**), both amide-functionalized surfactants clearly outperformed **1** as far as the binding affinity of the MINP was concerned.

Table 1. Binding data for MINPs (obtained by ITC unless indicated otherwise)[a]

Entry	MINP[b]	Guest	-Δ*G* (kcal/mol)	*N*	K_a (10^4 M^{-1})	-Δ*H* (kcal/mol)	TΔ*S* (kcal/mol)
1	$MINP_{1}$(**7**)	**7**	6.8	1.3 ± 0.2	12.8 ± 0.3 (15.3 ± 1.1)	4.7 ± 0.9	2.2
2	$MINP_{4a}$(**7**)	**7**	8.1	1.0 ± 0.1	90.4 ± 2.8 (99.3 ± 1.6)	7.99 ± 0.95	0.1
3	$MINP_{4b}$(**7**)	**7**	7.2	1.5 ± 0.1	46.6 ± 3.9 (40.2 ± 2.6)	4.66 ± 0.1	3.1
4	$MINP_{1}$(**8**)	**8**	6.6	1.0 ± 0.3	7.70 ± 0.30 (8.2 ± 1.0)	3.15 ± 1.0	2.8
5	$MINP_{4a}$(**8**)	**8**	7.7	0.5 ± 0.1	42.6 ± 0.8 (35.6 ± 2.1)	2.45 ± 0.24	5.2
6	$MINP_{4b}$(**8**)	**8**	6.2	0.8 ± 0.1	22.3 ± 1.2 (25.7 ± 1.9)	1.36 ± 0.4	5.9
7	$MINP_{1}$(**9**)	**9**	6.7	0.8 ± 0.1	12.0 ± 1.2 (11.0± 1.3)	2.15 ± 0.6	4.8
8	$MINP_{4a}$(**9**)	**9**	6.2	1.1 ± 0.1	34.0 ± 1.2 (33.0 ± 1.7)	3.28 ± 0.6	4.3
9	$MINP_{4b}$(**9**)	**9**	7.0	0.8 ± 0.2	14.7 ± 0.5 (21.7 ± 1.8)	3.15 ± 0.92	3.9
10	$MINP_{1:4a=1:3}$(**7**)	**7**	7.8	0.7 ± 0.1	51.6 ± 3.5	9.54 ± 0.15	-1.8
11	$MINP_{1:4a=1:1}$ (**7**)	**7**	7.5	1.5 ± 0.1	32.5 ± 2.7	3.80 ± 0.05	3.7
12	$MINP_{1:4a=3:1}$ (**7**)	**7**	6.9	1.4 ± 0.1	12.6 ± 1.4	1.3 ± 0.04	5.7
13	$MINP_{4a}$(**7**)	**8**	6.8	1.6 ± 0.1	9.40 ± 0.17	0.70 ± 0.03	6.1
14	$MINP_{4a}$(**7**)	**9**[c]	-	-	-	-	-
15	$MINP_{4a}$(**8**)	**7**	6.2	1.6 ± 0.1	9.07 ± 1.36	0.25 ± 0.02	6.5
16	$MINP_{4a}$(**8**)	**9**	6.5	0.7 ± 0.1	5.72 ± 0.13	1.6 ± 0.09	4.9
17	$MINP_{4a}$(**9**)	**7**[c]	-	-	-	-	-

18	$MINP_{4a}$(**9**)	**8**	5.2	1.4 ± 0.3	7.87 ± 0.95	7.4 ± 0.2	0.6

[a] The titrations were generally performed in duplicates in Millipore water and the errors between the runs were <20%. The binding constants in parentheses were from fluorescence titration and thus the number of binding sites and binding enthalpy/entropy were not available. [b] The subscript denotes the cross-linkable surfactant used in the MINP synthesis and the number in parentheses the template molecule. [c] Binding was too weak to be detected by ITC.

The same trend was maintained for templates **8** and **9** (Table 1, entries 4–6 and 7–9), with the binding affinity displaying a consistent order of $MINP_{4a}$ > $MINP_{4b}$ > $MINP_1$. Thus, the two amide-functionalized surfactants clearly worked better than the original **1** for the model templates, regardless of their substitution pattern. The data also suggest that hydrogen bonds between the template and the cross-linkable surfactants were important to the binding.

We also prepared nonimprinted nanoparticles from surfactant **1**, **4a**, and **4b**, respectively. The same synthetic procedure was followed except no template was used. ITC showed that none of the guest molecules (**7**–**9**) could bind the nonimprinted nanoparticles (Figure 12S–14S). The results further confirmed the molecular imprinting and ruled out nonspecific interactions between the MINPs and the guests.

If we compare the binding affinities of MINPs prepared from the same surfactant for different templates, $MINP_1$ was practically insensitive to the substitution pattern of the template, with ITC-measured K_a = 12.8, 7.70, and 12.0 × 10^4 M^{-1} for **7**, **8**, and **9**, respectively (Table 1, entries 1, 4, and 7). $MINP_{4a}$ and $MINP_{4b}$, on the other hand, showed a consistent trend in their affinities, i.e., **7** > **8** > **9** (Table 1, compare entries 2, 5, 8, or 3, 6, 9). Note that the different K_a values do NOT reflect the binding selectivity of the MINPs (which will be discussed later), as they are the binding constants between three different template molecules and their corresponding MINPs.

Overall, two consistent trends were observed for the amide-functionalized MINPs regarding their binding affinity: $MINP_{4a}$ > $MINP_{4b}$ for all three templates (**7**–**9**) and templates **7** > **8** > **9** for both MINPs. These results, first of all, suggest there is no special benefit in matching the distance between the ionic and the hydrogen-bonding functional group in the surfactant and the template. This is because

the better surfactant (**4a**) of the two has a shorter distance between these groups and the best template (**7**) among the three has the longest distance.

One possible reason for the observed binding trend of **7** > **8** > **9** is the depth of the hydrophobic dansyl group. Compound **7** has the dansyl and carboxylate *para* to each other. Since the carboxylate has to stay on the surface of the micelle/MINP, **7** is expected to have its dansyl deeper in the MINP hydrophobic core than either the *meta* (**8**) or *ortho* (**9**) derivative. When both hydrogen-bonding and hydrophobic interactions are involved in the guest binding, we need to maximize both interactions to have the highest binding affinity.[43] To engage in hydrogen-bonds, the sulfonamide of the template needs to be close to the amide groups in the final MINP. Such an arrangement seems easily achievable for all three templates, by their tilting to different degrees with the carboxylate anchored on the MINP surface. To maximize the hydrophobic interactions, however, dansyl needs to penetrate the amide layer and reach into the hydrocarbon core, and template **7** seems to have a clear advantage over the other two due to its *para* substitution.

Why didn't the substitution pattern of the template influence the binding of $MINP_1$, prepared from the amide-free surfactant? The most likely reason is the solvation of the sulfonamide group. Being highly hydrophilic, the sulfonamide can be "solvated" properly either by water or through interactions with the amide bonds of the surfactants. Since there are no amide groups in the micellar core of $MINP_1$, the only way for the sulfonamide to be properly solvated is to stay on the micellar surface, exposed to water. When both the carboxylate and sulfonamide need to stay on the micellar surface, the aminobenzoate moiety of the template is exposed to water and thus contributes little to binding. What is most important to the binding under such a circumstance are the hydrophobic interactions from burying the dansyl from solvent exposure and the electrostatic interactions between the oppositely charged host and guest—both are fairly constant among the three templates.

We also prepared MINPs using a mixture of **1** and **4a** in different ratios (Table 1, entries 10–12). The original idea was that, in doing so, the hydrogen bonds between **4a** and the template would be formed in a "background" (or microenvironment) of hydrocarbon and might be stronger. Essentially, surfactant **1**

would create a hydrocarbon-based micellar core, which could be drier and helpful to the hydrogen-bonding interactions between **4a** and the template. Instead, our data showed a monotonous decrease of K_a with decreasing **4a** in the MINP formulation (compare entries 2, 10, 11, 12, and 1), suggesting that the hypothesis was incorrect.

A key feature of molecularly imprinted polymers is their binding selectivity toward structural analogues. To understand this property, we titrated our MINPs with the "wrong" guest molecules, e.g., $MINP_{4a}$(**7**) with **8** and **9** and likewise for the other MINPs. Our imprinted cross-linked micelles showed good selectivity consistently. For example, $MINP_{4a}$(**7**) bound its template **7** most strongly among the three isomeric guests (entry 2). The binding constant decreased by nearly 10-fold for the *meta* derivative **8** (entry 13) and was undetectable for the *ortho* guest **9** (entry 14). For $MINP_{4a}$(**9**) imprinted against the *ortho* derivative, the strongest binding was observed for **9** as expected (entry 8). Binding for the *meta* derivative **8** was about 1/4 as strong (entry 18) and undetectable for the *para* derivative **7** (entry 17). For $MINP_{4a}$(**8**) imprinted against the *meta* derivative, its best guest was certainly its own template (entry 5) but, interestingly, both the *para* and *ortho* derivatives showed binding, albeit with a lower affinity (entries 15 and 16). These data suggest the MINPs overall were very selective and bind their own templates the best. In their binding of the "wrong" constitutional isomers, a mismatch of substitution by 1 (from 1,4 to 1,3; from 1,2 to 1,3; or from 1,3 to 1,2 or 1,4) gave weaker but measurable binding, whereas a mismatch by 2 (from 1,2 to 1,4 or vice versa) could not be tolerated at all.

Binding of Other Guests. The above studies gave us a good understanding of how amide-functionalized MINPs bind model guests containing hydrogen-bonding groups in the structure. Both $MINP_{4a}$ and $MINP_{4b}$ clearly outperformed the original $MINP_1$ without internal hydrogen-bonding capabilities. To see whether the advantage is maintained with other templates, we generated MINPs using **4a** (the best surfactant in this study) for four other templates (**10**–**13**). All four templates have been imprinted previously with surfactant **1**. Among the four templates, bile salt **10** had multiple hydrogen-bonding groups (hydroxyl and sulfonamide) arranged in a facially amphiphilic fashion.[32] 1-Naphthoic acid sodium salt **11** had a hydrocarbon aryl hydrophobe but no (heteroatom) hydrogen-

bonding functionalities in the hydrophobe (other than the carboxylate).[33] Naproxen and Indomethacin are both nonsteroidal anti-inflammatory drugs (NSAIDs), with Indomethacin **13** having a stronger hydrogen-bonding amide group in the midsection of the molecule than Naproxen **12**, which contains an ether.[36]

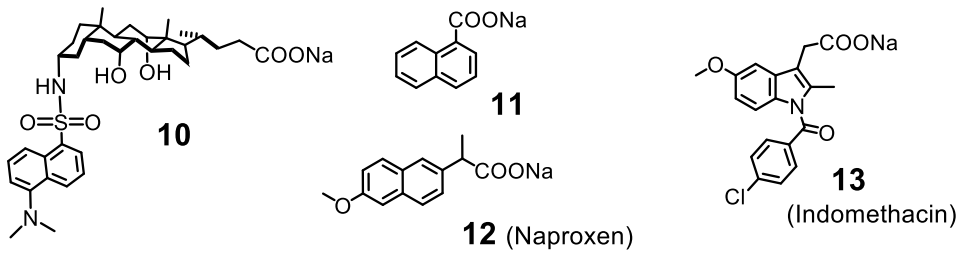

A quick glance of the binding data in Table 2 shows that the amide-containing surfactant (**4a**) was not always a winner. For the two NSAIDs (**12** and **13**), $MINP_{4a}$ showed 30–40% stronger binding than $MINP_1$, but for templates **10** and **11**, the opposite was true. Overall, the binding data are consistent with the earlier notion that templates with internal hydrogen-bonding functionalities benefit most from the amide-containing **4a**. For example, as far as internal hydrogen-bonding capabilities are concerned, templates **11**–**13** should follow the order of **11** < **12** < **13**, as the template possesses an increasing number of ether and amide. The relative binding constant of $MINP_{4a}$ to $MINP_1$ (i.e., K_{rel} in Table 2) increased steadily from 0.2 to 1.3 to 1.4 for the three templates.

Table 2. Binding data for MINPs obtained by ITC[a]

Entry	MINP	Guest	-Δ*G* (kcal/mol)	*N*	K_a (10^4 M^{-1})	K_{rel}[b]	-Δ*H* (kcal/mol)	TΔ*S* (kcal/mol)
1	$MINP_{4a}$(**10**)	**10**	8.3	0.9 ± 0.1	126 ± 6	0.4	7.67 ± 0.3	0.6
2	$MINP_1$(**10**)	**10**	8.9	1.0 ± 0.1	347 ± 23	1	33.1 ± 2.6	-24.2
3	$MINP_{4a}$(**11**)	**11**	6.8	0.7 ± 0.1	9.8 ± 0.6	0.2	5.67 ± 0.9	1.1
4	$MINP_1$(**11**)	**11**	7.7	1.1 ± 0.1	42.9 ± 1.3	1	6.7 ± 0.2	1.0

5	$MINP_{4a}$(**12**)	**12**	8.3	0.7 ± 0.1	115 ± 5	1.3	1.20 ± 0.14	7.1
6	$MINP_{1}$(**12**)	**12**	8.1	0.6 ± 0.1	91 ± 4	1	28.1 ± 6.0	-20.0
7	$MINP_{4a}$(**13**)	**13**	8.4	0.5 ± 0.1	140 ± 9	1.4	1.48 ± 0.18	6.9
8	$MINP_{1}$(**13**)	**13**	8.2	1.1 ± 0.1	98 ± 5	1	26.9 ± 1.0	-18.7

[a] Binding was measured in 50 mM Tris buffer (pH = 7.4). The titrations were generally performed in duplicates and the errors between the runs were <20%. The binding data for $MINP_{4a}$ were obtained in the current study and those for $MINP_{1}$ were taken from previous publications for templates **10**,[32] **11**,[33] and **12**–**13**.[36]

[b] K_{rel} is the binding affinity of $MINP_{4a}$ relative to $MINP_{1}$ for the same template.

Our model compounds **7**–**9** have stronger internal hydrogen-bonding capabilities than **11**–**13**, with the sulfonamide group possessing both hydrogen-bond donors and acceptors. Indeed, K_{rel} was even higher and was calculated to be 2.8 for **9**, 5.5 for **8**, and 7.1 for **7** from the binding data in Table 1. The continuous increase of K_{rel} from the *ortho* to *meta* to *para* template indicates that the template benefiting most from the amide-containing surfactant had its hydrogen-bonding sulfonamide deepest in the MINP hydrophobic core. The result is very reasonable: the deeper the hydrogen-bonding group into the hydrophobic core, the more it can be shielded from water and the stronger the hydrogen bonds will be.

Once the above picture is made clear, it becomes quite obvious why the amide-functionalized surfactant did not help bile salt derivative **10**. Although the template has many hydrogen-bonding groups, they are all on the α face of the cholate, opposite to the hydrophobic β face. Because hydrophobic interactions are key to the incorporation of the hydrophobic template into the micelle, **10** might lie flat on the micellar surface, having the hydrophilic face toward water and hydrophobic face toward the interior of the micelle. With such an orientation, the amide groups inside the micelle of **4a** would have little chance interacting with the template through hydrogen bonds. To make things worse, the layer of amide bonds near the surface of the micelle would weaken the hydrophobic interactions between **10** and the micelle (ultimately $MINP_{4a}$). This could be the reason why $MINP_{4a}$(**10**) displayed much weaker binding toward the template than $MINP_{1}$(**10**) (Table 2, entries 1 and 2). The same could the reason why template **11** was bound more strongly by $MINP_{1}$(**11**) than $MINP_{4a}$(**11**).

Conclusions

Our study so far gives a consistent mechanistic picture in the binding of amide-functionalized MINPs. Surfactant **4a** with two methylene groups between the tripropargylammonium headgroup and the amide outperformed surfactant **4b** with four methylene groups. In general, **4a** was most effective in the molecular imprinting of template molecules with strong hydrogen-bonding functionalities but the location of these functional groups was also critical. Overall, the binding between amide-functionalized MINPs and the templates are driven by a combination of hydrophobic and hydrogen-bonding interactions (in addition to electrostatic interactions in our case). To maximize the hydrophobic interactions, the template/guest molecule needs to possess a sizable hydrophobe but it is best for the hydrophobe to penetrate the amide layer to reach into the hydrophobic core of the MINP. To maximize the hydrogen-bonding interactions, the templates should possess strong hydrogen-bonding groups that can favorably interact with the internal amide bonds geometrically.

The most significant learning in this work is a detailed understanding of how different intermolecular interactions can be used rationally to enhance the binding of molecularly imprinted nanoparticle receptors. MIPs are traditionally intractable cross-linked polymers that prohibit detailed study of their binding mechanisms. The water-solubility, nanodimension, and fine-tunability of our MINPs gave us tremendous opportunities to examine the details of binding. The knowledge generated will enable better designs of these protein-mimetic "plastic antibodies" that could find many applications in chemistry and biology.

Experimental Section

Syntheses of compounds **1**, **2**, **3**, **4**, and **10** were previously reported.[32]

***N-(2-Aminoethyl)-5-hydroxyundecanamide* (5a).** δ-Undecalactone (1.0 mL, 5 mmol) and ethylenediamine (1.5 g, 25 mmol) were stirred at room temperature for 4 h. The excess amine was removed by co-evaporation with methanol (5 × 2 mL) in a rotary evaporator. The residual was combined with ether (50 mL) and kept overnight. The precipitate was recovered by vacuum filtration

and washed with ether (3 × 30 mL) to afford a white powder (1.10 g, 84 %). ^{1}H NMR (400 MHz, $CDCl_3$, δ): 6.11 (br, 1H, N-H), 3.62 (m, 1H), 3.30 (t, *J* = 8.0 Hz, 2H), 2.84 (t, *J* = 8.0 Hz, 2H), 2.37 (t, *J* = 8.0 Hz, 2H), 1.88 (m, 2H), 1.67 (m, 2H), 1.43 (m, 2H), 1.26 (m, 8H), 0.85 (t, *J* = 8.0 Hz, 3H). ^{13}C NMR (100 MHz, CD_3OD, δ): 176.5, 71.7, 42.0, 41.6, 38.3, 33.9, 33.3, 32.8, 30.6, 30.3, 26.6, 23.5, 14.2. ESI-QTOF-HRMS (*m/z*): $[M+H]^+$ calcd for $C_{13}H_{28}N_2O_2$ 245.2224; found, 245.2219.

***N*-(2-(5-hydroxyundecanamido)ethyl)-*N*,*N*-di(prop-2-yn-1-yl)prop-2-yn-1-aminium bromide (6a).** A mixture of **5a** (0.80 g, 3.3 mmol) and $NaHCO_3$ (0.87 g, 10.82 mmol) in CH_3CN (2.00 mL) was stirred at 70 °C while a solution of propargyl bromide (1.0 mL, 10.82 mmol) in dry CH_3CN (2.0 mL) was added dropwise over 10 min. The mixture was stirred for 16 h at 70 °C before another batch of propargyl bromide (0.33 mL) and $NaHCO_3$ (0.30 g) were added. The mixture was stirred for another 4 h. The inorganic salts were removed by filtration. After the solvent was removed by rotary evaporation, the residue was purified by column chromatography over silica gel using 30:1 dichloromethane/methanol as the eluent to afford a yellowish oil (0.65 g, 77 %). ^{1}H NMR (400 MHz, $CDCl_3$, δ): 8.52 (br, 1H, N-H), 4.82 (m, 1H), 4.78 (s, 6H), 3.93 (t, *J* = 8.0 Hz, 2H), 3.84 (t, *J* = 8.0 Hz, 2H), 3.59 (t, *J* = 8.0 Hz, 2H), 3.13 (s, 3H), 2.36 (m, 2H), 1.77 (m, 2H), 1.46 (m, 4H), 1.26 (m, 6H), 0.88 (t, *J* = 8.0 Hz, 3H) ppm. ^{13}C NMR (100 MHz, $CDCl_3$, δ): 175.2, 83.1, 71, 70, 58.5, 50.8, 37.6, 36.7, 36, 34.1, 31.8 29.4, 25.8, 22.64, 21.5, 14.1 ppm. ESI-QTOF-HRMS (*m/z*): $[M-Br]^+$ calcd for $C_{22}H_{35}N_2O_2$, 359.2693; found, 359.2696.

***N*-(2-(5-(methacryloyloxy)undecanamido)ethyl)-*N*,*N*-di(prop-2-yn-1-yl)prop-2-yn-1-aminium chloride (4a).** A solution of methacryloyl chloride (0.1 mL, 1.0 mmol) in dry CH_2Cl_2 (0.5 mL) was added dropwise over 10 min to a solution of **6a** (0.193 g, 0.60 mmol) and diisopropylethylamine (DIPEA , 0.14 mL. 1.5 mmol) in dry CH_2Cl_2 (10 mL) at 0 °C. After 30 min at 0 °C, the mixture was stirred for 5 h at room temperature before a second batch of methacryloyl chloride (0.05 mL, 0.5 mmol) was added. A third batch of methacryloyl chloride (0.05 mL, 0.5 mmol) was added after another 5 h and the mixture was stirred at 40 °C for additional 5 h. After the solvent was removed by rotary evaporation,

the residue was purified by column chromatography over silica gel using 4:1 ethyl acetate/methanol as the eluent to afford a yellowish oil (0.10 g, 45%).^{1}H NMR (400 MHz, $CDCl_3$, δ): 8.44 (br, 1H, N-H), 6.1(s,1H), 5.5 (s, 1H), 4.90 (m, 1H), 4.80 (s, 6H), 4.10 (t, *J* = 8.0 Hz, 2H), 3.90 (t, *J* = 8.0 Hz, 2H), 3.84 (t, *J* = 8.0 Hz, 2H),3.03 (s, 3H), 2.30 (m, 2H), 2.04 (m, 2H), 1.92 (s, 3H), 1.62 (m, 4H), 1.26 (m, 6H), 0.88 (t, *J* = 8.0 Hz, 3H) ppm.^{13}C NMR (100 MHz, $CDCl_3$, δ): 174.5, 167.3, 136.6, 125.2, 82.9, 74.3, 69.8, 60.4, 58.8, 50.8, 37.8, 35.9, 34, 31.7, 29.2, 25.2, 22.5,21.3, 18.4, 14 ppm. ESI-QTOF-HRMS (*m/z*): $[M-Cl]^+$ calcd for $C_{26}H_{39}N_2O_3$, 427.2955; found, 427.2961.

***N*-(4-aminobutyl)-5-hydroxyundecanamide (5b).** δ-Undecalactone (3.0 mL, 15 mmol) and 1,4-diaminobutane (6.6 g, 75 mmol) were stirred for 4 h at room temperature. The excess amine was removed by co-evaporation with methanol (5 × 4 mL) in a rotary evaporator. The residual was combined with ether (100 mL) and kept overnight. The precipitate was recovered by vacuum filtration and washed with ether (3 × 30 mL) to afford a white powder (3.5 g, 80 %). ^{1}H NMR (400 MHz, $CDCl_3$, δ): 6.0 (br, 1H, N-H), 3.50 (m, 1H), 3.18 (t, *J* = 8.0 Hz, 2H), 2.66 (t, *J* = 8.0 Hz, 2H), 2.14 (t, *J* = 8.0 Hz, 2H), 1.67 (m, 6H), 1.44 (m, 4H), 1.35 (m, 4H), 1.20 (m, 4H), 0.80 (t, *J* = 8.0 Hz, 3H) ppm.^{13}C NMR (100 MHz, CD_3OD, δ): 175.9, 71.8, 41.3, 39.7, 38.2, 37.6,36.9, 32.9, 30.3, 29.1, 27.5, 26.6, 23.5, 23.2, 14.2 ppm. ESI-QTOF-HRMS (*m/z*): $[M-Br]^+$ calcd for $C_{26}H_{39}N_2O_3$, 273.2537; found, 273.2541.

4-(5-Hydroxyundecanamido)-*N*,*N*,*N*-tri(prop-2-yn-1-yl)butan-1-aminium bromide (6b). A mixture of **5b** (0.40 g, 1.4 mmol) and $NaHCO_3$ (0.41 g, 5.7 mmol) in CH_3CN (5.00 mL) was stirred at 70 °C while a solution of propargyl bromide (0.46 mL, 5.7 mmol) in dry CH_3CN (2.0 mL) was added dropwise over 10 min. The mixture was stirred for 16 h at 70 °C before another batch of propargyl bromide (0.2 mL) and $NaHCO_3$ (0.30 g) were added. The mixture was stirred for another 4 h. The inorganic salts were removed by filtration. After the solvent was removed by rotary evaporation, the residue was purified by column chromatography over silica gel using 7:3 ethyl acetate/methanol as the eluent to afford a yellowish oil (0.40 g, 72 %). ^{1}H NMR (400 MHz, $CDCl_3$, δ): 7.68 (br, 1H, N-H), 4.72 (s, 6H), 3.71 (t, *J* = 8.0 Hz, 2H), 3.60 (t, *J* = 8.0 Hz, 2H), 3.58 (m, 1H), 3.2 (m, 4H), 3.2 (m,4H), 3.03 (s,

3H), 2.15 (m, 2H), 1.76 (m, 2H), 1.70 (m, 4H), 1.40 (m, 4H), 0.86 (t, J = 8.0 Hz, 3H) ppm. ^{13}C NMR (100 MHz, $CDCl_3$, δ): 175.5, 82.6, 71, 70.5, 69.9, 60.5, 50.3, 37.8, 37.3, 36.5, 36.1, 31.7, 29.5, 29.3, 25.9, 25.7, 22.5, 21.9, 3.9 ppm. ESI-QTOF-HRMS (*m/z*): $[M\text{-}Br]^+$ calcd for $C_{24}H_{39}N_2O_2$ 387.3006; found, 387.2999.

4-(5-(Methacryloyloxy)undecanamido)-*N*,*N*,*N*-tri(prop-2-yn-1-yl)butan-1-aminium chloride (4b). A solution of methacryloyl chloride (0.5 mL, 4.12 mmol) in dry CH_2Cl_2 (0.5 mL) was added dropwise over 10 min to a solution of **6b** (0.71 g, 1.82 mmol) and DIPEA (0.45 mL, 4.5 mmol) in dry CH_2Cl_2 (30 mL) at 0 °C. After 30 min at 0 °C, the mixture was stirred for 5 h at room temperature before a second batch of methacryloyl chloride (0.23 mL, 1.88 mmol) was added. The mixture was stirred at 40 °C for additional 8h. After the solvent was removed by rotary evaporation, the residue was purified by column chromatography over silica gel using 4:1 ethyl acetate/methanol as the eluent to afford a yellowish oil (0.47 g, 56%).^{1}H NMR (400 MHz, $CDCl_3$ δ): 6.0 (s,1H), 5.5 (s, 1H), 4.77 (s, 6H), 4.08 (t, J = 8.0 Hz, 2H), 3.60 (m, 2H), 2.81 (s, 3H) ,1.98 (m, 4H), 1.89 (s, 3H), 1.61 (m, 4H), 1.58 (m, 6H), 1.52 (m, 8H), 0.88 (t, J = 8.0 Hz, 3H) ppm. ^{13}C NMR (100 MHz, $CDCl_3$ & CH^3OD, δ): 180.30, 171.57, 145.8, 129.4, 86.0, 78.1, 73.7, 58.6, 54.2, 46.8, 42.0, 37.8, 35.8, 33.0, 30.0, 29.1, 26.4, 24.3, 22.7, 22.4, 21.1, 17.8 ppm. ESI-QTOF-HRMS (*m/z*): $[M\text{-}Cl]^+$ calcd for $C_{28}H_{43}N_2O_3$ 455.3268; found, 455.3255.

Methyl 4-aminobenzoate (7a).[44] To a solution of 4-amino benzoic acid (2.0 g, 14.6 mmol) in 40 mL MeOH, concentrated H_2SO_4 (1.75 mL, 33 mmol) was added dropwise. After the mixture was heated to reflux for 8 h, the solvent was removed under reduced pressure. Water (25 mL) was added and the solution pH was adjusted to 3 with 2 M NaOH. The precipitate formed was collected by filtration and washed with water (20 mL) to afford a white solid (1.94 g, 86%). ^{1}H NMR (400 MHz, $CDCl_3$, δ): 7.85 (dd, J = 8 & 4 Hz, 2H), 6.64 (dd, J = 8 & 4 Hz, 2H), 4.03 (br, NH_2), 3.85 (s, 3H).

Methyl 4-((5-(dimethylamino)naphthalene)-1-sulfonamido)benzoate (7b).[45] To a solution of dansyl chloride (0.09 g, 0.33 mmol) in dry dichloromethane (20 mL) was added to a solution of

compound **7a** (0.05 g, 0.33 mmol) and triethylamine (0.07 mL, 0.66 mmol) in 3 mL dry dichloromethane. The mixture was stirred at room temperature for 6 h under N_2. After the solvent was removed by rotary evaporation, the residue was purified by column chromatography over silica gel using 2:1 ethyl acetate/hexane as the eluent to afford a white powder (0.10 g, 77%).^{1}H NMR (400 MHz, $CDCl_3$, δ): 8.53 (d, *J* = 8 Hz, 1H), 8.21 (d, *J* = 8 Hz, 1H), 7.77 (dd, *J* = 8 & 4 Hz, 2H), 7.41 (dd, *J* = 8 & 4 Hz, 2H), 3.84 (s, 3H), 2.81 (s, 6H).

4-((5-(Dimethylamino)naphthalene)-1-sulfonamido)benzoic acid (7c).[46] LiOH (5.0 mL, 2 M) was added to a solution of compound **7b** (0.17 g, 0.44 mmol) in MeOH (15 mL).The mixture was stirred for 12 h at room temperature. The mixture was concentrated under reduced pressure and acidified by 2 M HCl. The precipitate formed was collected by filtration and dried in air to afford a white powder (0.10 g, 77%). To obtain the sodium salt of this compound, the above acid was mixed with saturated sodium bicarbonate (2.0 mL) and methanol (5 mL). The reaction mixture was stirred for 2 h. After the solvents were removed by rotary evaporation, the residue was dissolved in methanol (5 mL). The solution was filtered and then concentrated by rotary evaporation to give the sodium salt as a white powder. ^{1}H NMR (400 MHz, CD_3OD, δ): 8.81 (d, *J* = 8 Hz, 1H), 8.67 (d, *J* = 8 Hz, 1H), 8.56 (d, *J* = 8 Hz, 1H), 8.03 (dd, *J* = 8 & 4 Hz, 2H), 7.85 (m, 2H),7.55 (d, *J* = 8 Hz, 1H), 7.35 (dd, *J* = 8 & 4 Hz, 2H), 3.13 (s, 6H).

Methyl 3-aminobenzoate (8a).[47] To a solution of 3-amino benzoic acid (3.0 g, 22 mmol) in 40 mL MeOH, concentrated H_2SO_4 (2.5 mL, 47 mmol) was added dropwise. After the mixture was heated to reflux for 8 h, the solvent was removed under reduced pressure. Water (25 mL) was added and the solution pH was adjusted to 3 with 2 M NaOH. The precipitate formed was collected by filtration and washed with water (20 mL) to afford a white solid (2.71g, 82%).^{1}H NMR (400 MHz, $CDCl_3$, δ): 7.42 (dd, *J* = 8 & 4 Hz, 2H), 7.35 (s, 1H), 7.21 (t, *J* = 8 Hz, 2H), 6.85 (dd, *J* = 8 & 4 Hz, 2H), 3.89 (s, 3H).

Methyl 3-((5-(dimethylamino)naphthalene)-1-sulfonamido)benzoate (8b).[48] To a solution of dansyl chloride (0.3 g, 1.1 mmol) in dry dichloromethane (20 mL) was added to a solution of compound

8a (0.15 g, 1.0 mmol) and triethylamine (0.22 mL, 2.0 mmol) in 3 mL dry dichloromethane. The mixture was stirred at room temperature for 6 h under N_2. After the solvent was removed by rotary evaporation, the residue was purified by column chromatography over silica gel using 2:1 ethyl acetate/hexane as the eluent to afford a white powder (0.10 g, 77%). ^{1}H NMR (400 MHz, $CDCl_3$, δ): 8.6 (d, *J* = 8 Hz, 1H), 8.3 (d, *J* = 8 Hz, 1H), 7.01 (m, 2H), 7.79 (d, *J* = 8 Hz, 1H), 7.56 (dd, *J* = 8 & 4 Hz, 1H), 7.46 (s, 1H), 7.20 (m, 1H), 7.20 (m, 2H), 5.30 (s, 3H), 2.89 (s, 6H).

3-((5-(Dimethylamino)naphthalene)-1-sulfonamido)benzoic acid (8c).[47] LiOH (5.0 mL, 2 M) was added to a solution of compound **8b** (0.17 g, 0.44 mmol) in MeOH (15 mL). The mixture was stirred for 12 h at room temperature. The mixture was concentrated under reduced pressure and acidified by 2 M HCl. The precipitate was collected by filtration and dried in air to afford a white powder (0.14 g, 93%). To obtain the sodium salt of this compound, the above acid was mixed with saturated sodium bicarbonate (2.0 mL) and methanol (5 mL). The reaction mixture was stirred for 2 h. After the solvents were removed by rotary evaporation, the residue was dissolved in methanol (5 mL). The solution was filtered and then concentrated by rotary evaporation to give the sodium salt as a white powder.^{1}H NMR (600 MHz, CD_3OD, δ): 8.83 (d, *J* = 8 Hz, 1H), 8.57 (d, *J* = 8 Hz, 1H), 8.41 (m, 1H), 8.21 (m, 2H), 7.49 (m, 2H), 7.24 (m, 2H), 7.06 (m, 1H), 6.95 (t, *J* = 8 Hz, 1H), 2.89 (s, 3H), 2.86(s, 3H).

Methyl 2-aminobenzoate (9a).[49] To a solution of 2-amino benzoic acid (2.0 g, 14.6 mmol) in 30 mL MeOH, concentrated H_2SO_4 (1.6 mL, 30 mmol) was added dropwise. After the mixture was heated to reflux for 8 h, the solvent was removed under reduced pressure. Water (20 mL) was added and the solution pH was adjusted to 3 with 2 M NaOH. The precipitate formed was collected by filtration and washed with water (20 mL) to afford a white solid (2.10 g, 95%). ^{1}H NMR (400 MHz, $CDCl_3$, δ): 7.79 (d, *J* = 8 Hz, 2H), 7.18 (t, *J* = 8 Hz, 1H), 6.53 (m, 2H), 3.72 (s, 3H).

Methyl 2-((5-(dimethylamino)naphthalene)-1-sulfonamido)benzoate (9b).[49] To a solution of dansyl chloride (0.22 g, 0.8 mmol) in dry dichloromethane (15 mL) was added to a solution of

compound **9a** (0.12 g, 0.8 mmol) and triethylamine (0.17 mL, 1.6 mmol) in 3 mL dry dichloromethane. The mixture was stirred at room temperature for 6 h under N_2. After the solvent was removed by rotary evaporation, the residue was purified by column chromatography over silica gel using 2:1 ethyl acetate/hexane as the eluent to afford a white powder (0.25 g, 83%). ^{1}H NMR (400 MHz, $CDCl_3$, δ):11.1 (br, 1H), 8.5 (m, 1H), 8.35 (3, 2H), 7.84 (m, 1H), 7.59 (m, 1H), 7.50 (m, 2H), 7.36 (m, 1H), 7.20 (m, 1H), 6.92 (m, 1H), 3.85 (s, 6H), 2.87 (s, 3H).

2-((5-(Dimethylamino)naphthalene)-1-sulfonamido)benzoic acid (9c).[49] LiOH (5.0 mL, 2 M) was added to a solution of compound **9b** (0.2 g, 0.40 mmol) in MeOH (15 mL). The mixture was stirred for 12 h at room temperature. The mixture was concentrated under reduced pressure and acidified by 2 M HCl. The precipitate was collected by filtration and dried in air to afford a white powder (0.14 g, 93%). To obtain the sodium salt of this compound, the above acid was mixed with saturated sodium bicarbonate (2.0 mL) and methanol (5 mL). The reaction mixture was stirred for 2 h. After the solvents were removed by rotary evaporation, the residue was dissolved in methanol (5 mL). The solution was filtered and then concentrated by rotary evaporation to give the sodium salt as a white powder. ^{1}H NMR (600 MHz, $CDCl_3$, δ): 11.1 (br, 1H), 8.5 (m, 1H), 8.35 (3, 2H), 7.84 (m, 1H), 7.59 (m, 1H), 7.50 (m, 2H), 7.36 (m, 1H), 7.20 (m, 1H), 6.92 (m, 1H), 3.85 (s, 6H).

Preparation of Molecularly Imprinted Nanoparticles (MINPs). To a micellar solution of compound **4a** (10.2 mg, 0.02 mmol) in D_2O (2.0 mL), divinylbenzene (DVB, 2.8 μL, 0.02 mmol), compound **7** in D_2O (10 μL of a solution of 15.68 mg/mL, 0.0004 mmol), and 2,2-dimethoxy-2-phenylacetophenone (DMPA,10 μL of a 12.8 mg/mL solution in DMSO, 0.0005 mmol) were added. (D_2O instead of H_2O was used in the preparation so that the cross-linking and polymerization of the micelles could by monitored by ^{1}H NMR spectroscopy) The mixture was subjected to ultrasonication for 10 min before compound **2** (4.13 mg, 0.024 mmol), $CuCl_2$ (10 μL of a 6.7 mg/mL solution in D_2O, 0.0005 mmol), and sodium ascorbate (10 μL of a 99 mg/mL solution in D_2O, 0.005 mmol) were added. After the reaction mixture was stirred slowly at room temperature for 12 h, compound **3** (10.6 mg, 0.04

mmol), $CuCl_2$ (10 μL of a 6.7 mg/mL solution in D_2O, 0.0005 mmol l), and sodium ascorbate (10 μL of a 99 mg/mL solution in D_2O, 0.005 mmol) were added. After being stirred for another 6 h at room temperature, the reaction mixture was transferred to a glass vial, purged with nitrogen for 15 min, sealed with a rubber stopper, and irradiated in a Rayonet reactor for 12 h. ^1H NMR spectroscopy was used to monitor the progress of reaction. The reaction mixture was poured into acetone (8 mL). The precipitate was collected by centrifugation and washed with a mixture of acetone/water (5 mL/1 mL) three times. The crude produce was washed by methanol/acetic acid (5 mL/0.1 mL) three times until the emission peak at 480 nm (for the dansyl) disappeared and then with excess methanol. The off white powder was dried in air to afford the final MINPs (12 mg, 70%).

Determination of Critical Micelle Concentration (CMC) of Surfactants. A typical procedure is as follows. A stock solution was prepared by adding surfactant **4a** (10.2 mg, 0.02 mmol) to 2.0 mL of an aqueous solution of pyrene (1.0×10^{-7} M). To 11 separate vials, 100, 90, 80, 70, 60, 50, 40, 30, 20, 15, 10, and 5 μL of the above stock solution were added. Millipore water was added to each vial to make the total volume 2.0 mL. Fluorescence spectra were recorded with the excitation wavelength at 336 nm. The final results were based on duplicate experiments with separately prepared solutions.

Determination of Binding Constants by Fluorescence Titration. A typical procedure is as follows. A stock solution containing $MINP_1$(**7**) (150 μM) was prepared in Millipore water. Aliquots (2.0 μL) of the MINP stock solution were added to 2.00 mL of the solution of **7** in Millipore water (0.2 μM). After each addition, the sample was allowed to sit for 1 min at room temperature before the fluorescence spectrum was collected. The excitation wavelength (λ_{ex}) was 340 nm. The excitation slit width was 10 nm, and the emission slit width was 10 nm.

Determination of Binding Constants by ITC. The determination of binding constants by ITC followed standard procedures.[50-52] In general, a solution of an appropriate guest in Millipore water was injected in equal steps into 1.43 mL of the corresponding MINP in the same solution. The top panel shows the raw calorimetric data. The area under each peak represents the amount of heat generated at each ejection and is plotted against the molar ratio of the MINP to the guest. The smooth solid line is the

best fit of the experimental data to the sequential binding of *N* binding site on the MINP. The heat of dilution for the guest, obtained by titration carried out beyond the saturation point, was subtracted from the heat released during the binding. Binding parameters were auto-generated after curve fitting using Microcal Origin 7.

ASSOCIATED CONTENT

Supporting Information

The Supporting Information is available free of charge on the ACS Publications website.

ITC titration curves, additional figures, and NMR spectra of key compounds (PDF).

AUTHOR INFORMATION

Corresponding Author

*E-mail: zhaoy@iastate.edu

Acknowledgments

We thank the National Institute of General Medical Sciences of the National Institutes of Health (R01GM113883) and NSF (DMR-1464927) for financial support of this research

Notes

The authors declare no competing financial interest.

References

(1) Atwood, J. L.; Lehn, J. M. *Comprehensive Supramolecular Chemistry*; Pergamon: New York, 1996.

(2) Steed, J. W.; Gale, P. A. *Supramolecular Chemistry: From Molecules to Nanomaterials*; Wiley: Weinheim, 2012.

(3) Schneider, H.-J.; Yatsimirsky, A. K. *Principles and methods in supramolecular chemistry*; Wiley: New York, 2000.

(4) Wulff, G. *Angew. Chem. Int. Ed. Engl.* **1995**, *34*, 1812.

(5) Wulff, G. *Chem. Rev.* **2001**, *102*, 1.

(6) Haupt, K.; Mosbach, K. *Chem. Rev.* **2000**, *100*, 2495.

(7) Ye, L.; Mosbach, K. *Chem. Mater.* **2008**, *20*, 859.

(8) Shea, K. J. *Trends Polym. Sci.* **1994**, *2*, 166.

(9) Sellergren, B. *Molecularly imprinted polymers: man-made mimics of antibodies and their applications in analytical chemistry*; Elsevier: Amsterdam, 2001.

(10) Komiyama, M. *Molecular imprinting: from fundamentals to applications*; Wiley-VCH: Weinheim, 2003.

(11) Yan, M.; Ramström, O. *Molecularly imprinted materials: science and technology*; Marcel Dekker: New York, 2005.

(12) Alexander, C.; Andersson, H. S.; Andersson, L. I.; Ansell, R. J.; Kirsch, N.; Nicholls, I. A.; O'Mahony, J.; Whitcombe, M. J. *J. Mol. Recognit.* **2006**, *19*, 106.

(13) Sellergren, B.; Hall, A. J. In *Supramol Chem*; John Wiley & Sons, Ltd: 2012.

(14) Haupt, K.; Ayela, C. *Molecular Imprinting*; Springer: Heidelberg ; New York, 2012.

(15) Zimmerman, S. C.; Wendland, M. S.; Rakow, N. A.; Zharov, I.; Suslick, K. S. *Nature* **2002**, *418*, 399.

(16) Zimmerman, S. C.; Zharov, I.; Wendland, M. S.; Rakow, N. A.; Suslick, K. S. *J. Am. Chem. Soc.* **2003**, *125*, 13504.

(17) Sellergren, B. *Angew. Chem. Int. Ed.* **2000**, *39*, 1031.

(18) Wu, X.; Carroll, W. R.; Shimizu, K. D. *Chem. Mater.* **2008**, *20*, 4335.

(19) Zimmerman, S. C.; Lemcoff, N. G. *Chem. Commun.* **2004**, 5.

(20) Li, Z.; Ding, J.; Day, M.; Tao, Y. *Macromolecules* **2006**, *39*, 2629.

(21) Hoshino, Y.; Kodama, T.; Okahata, Y.; Shea, K. J. *J. Am. Chem. Soc.* **2008**, *130*, 15242.

(22) Priego-Capote, F.; Ye, L.; Shakil, S.; Shamsi, S. A.; Nilsson, S. *Anal. Chem.* **2008**, *80*, 2881.

(23) Cutivet, A.; Schembri, C.; Kovensky, J.; Haupt, K. *J. Am. Chem. Soc.* **2009**, *131*, 14699.

(24) Yang, K. G.; Berg, M. M.; Zhao, C. S.; Ye, L. *Macromolecules* **2009**, *42*, 8739.

(25) Zeng, Z. Y.; Patel, J.; Lee, S. H.; McCallum, M.; Tyagi, A.; Yan, M. D.; Shea, K. J. *J. Am. Chem. Soc.* **2012**, *134*, 2681.

(26) Ma, Y.; Pan, G. Q.; Zhang, Y.; Guo, X. Z.; Zhang, H. Q. *Angew. Chem. Int. Ed.* **2013**, *52*, 1511.

(27) Çakir, P.; Cutivet, A.; Resmini, M.; Bui, B. T.; Haupt, K. *Adv. Mater.* **2013**, *25*, 1048.

(28) Zhang, Y.; Deng, C.; Liu, S.; Wu, J.; Chen, Z.; Li, C.; Lu, W. *Angew. Chem. Int. Ed.* **2015**, *54*, 5157.

(29) Chen, L. X.; Xu, S. F.; Li, J. H. *Chem. Soc. Rev.* **2011**, *40*, 2922.

(30) Gunasekara, R. W.; Zhao, Y. *J. Am. Chem. Soc.* **2015**, *137*, 843.

(31) Gunasekara, R. W.; Zhao, Y. *Chem. Commun.* **2016**, *52*, 4345.

(32) Awino, J. K.; Zhao, Y. *J. Am. Chem. Soc.* **2013**, *135*, 12552.

(33) Awino, J. K.; Zhao, Y. *Chem. Commun.* **2014**, *50*, 5752.

(34) Awino, J. K.; Zhao, Y. *Chem.-Eur. J.* **2015**, *21*, 655.

(35) Awino, J. K.; Hu, L.; Zhao, Y. *Org. Lett.* **2016**, *18*, 1650.

(36) Awino, J. K.; Zhao, Y. *ACS Biomater. Sci. Eng.* **2015**, *1*, 425.

(37) Zhang, S.; Zhao, Y. *Macromolecules* **2010**, *43*, 4020.

(38) Peng, H.-Q.; Chen, Y.-Z.; Zhao, Y.; Yang, Q.-Z.; Wu, L.-Z.; Tung, C.-H.; Zhang, L.-P.; Tong, Q.-X. *Angew. Chem. Int. Ed.* **2012**, *51*, 2088.

(39) Kalyanasundaram, K.; Thomas, J. K. *J. Am. Chem. Soc.* **1977**, *99*, 2039.

(40) Zhang, S.; Zhao, Y. *J. Am. Chem. Soc.* **2010**, *132*, 10642.

(41) Li, Y. H.; Chan, L. M.; Tyer, L.; Moody, R. T.; Himel, C. M.; Hercules, D. M. *J. Am. Chem. Soc.* **1975**, *97*, 3118.

(42) Schmidtchen, F. P. In *Supramol Chem*; John Wiley & Sons, Ltd: 2012.

(43) Electrostatic interactions between the positively charged MINP and the negatively charged template should be fairly constant within the series and thus not discussed here.

(44) Takamatsu, D.; Fukui, K.-i.; Aroua, S.; Yamakoshi, Y. *Org. Biomol. Chem.* **2010**, *8*, 3655.

(45) Wu, H.; Zhou, P.; Wang, J.; Zhao, L.; Duan, C. *New J. Chem.* **2009**, *33*, 653.

(46) Himel, C. M.; Aboul-Saad, W. G.; Uk, S. *J. Agric. Food Chem.* **1971**, *19*, 1175.

(47) Hejesen, C.; Petersen, L. K.; Hansen, N. J. V.; Gothelf, K. V. *Org. Biomol. Chem.* **2013**, *11*, 2493.

(48) Sosic, I.; Turk, S.; Sinreih, M.; Trost, N.; Verlaine, O.; Amoroso, A.; Zervosen, A.; Luxen, A.; Joris, B.; Gobec, S. *Acta Chim. Slov.* **2012**, *59*, 380.

(49) Carrillo-Arcos, U. A.; Rojas-Ocampo, J.; Porcel, S. *Dalton transactions (Cambridge, England : 2003)* **2016**, *45*, 479.

(50) Wiseman, T.; Williston, S.; Brandts, J. F.; Lin, L. N. *Anal. Biochem.* **1989**, *179*, 131.

(51) Jelesarov, I.; Bosshard, H. R. *J. Mol. Recognit.* **1999**, *12*, 3.

(52) Velazquez-Campoy, A.; Leavitt, S. A.; Freire, E. *Methods Mol. Biol.* **2004**, *261*, 35.

TOC graphic